Shielding effect of a nano-circular inclusion acting on semi-infinite wedge cracks*

Song Hao-Peng(宋豪鹏)† and Gao Cun-Fa(高存法)

College of Aerospace Engineering, State Key Laboratory of Mechanics and Control of Mechanical Structures, Nanjing University of Aeronautics & Astronautics, Nanjing 210016, *China*

(Received 6 April 2012; revised manuscript received 7 August 2012)

The model of a screw dislocation near a semi-infinite wedge crack tip inside a nano-circular inclusion is proposed to investigate the shielding effect of nano inclusions acting on cracks. Utilizing the complex function method, the closed-form solutions of the stress fields in the matrix and the inclusion region are derived. The stress intensity factor, the image force, as well as the critical loads for dislocation emission are discussed in detail. The results show that the nano inclusion not only enhances the shielding effect exerted by the dislocation, but also provides a shielding effect itself. Moreover, dislocations may be trapped in the nano inclusion even if the matrix is softer than the inclusion. This helps the dislocation shield crack, and reduces the dislocation density within the matrix.

Keywords: screw dislocation, wedge crack, nano inclusion, shielding effect

PACS: 62.20.mm, 62.20.mt, 62.23.Pq **DOI:** 10.1088/1674-1056/22/1/016201

1. Introduction

It is well known that dislocations in the vicinity of a crack tip play an important role in fracture mechanics. Therefore, the elastic interaction between dislocations and cracks has been extensively studied by many theoretical and experimental researchers.[1–10] The stress field, image force and strain energy of dislocation, and the stress intensity factor at the crack tip are the major concerns in these investigations. When the plastic deformation occurs around a crack tip, the stress field in the vicinity of the tip changes. One of the mechanisms, the dislocation emitted from the crack tip into the plastic zone, can reduce the stress intensity factor at the crack tip. This phenomenon is known as the dislocation shielding effect.[11] Rice and Thomson[12] obtained a quantitative criterion for ductile verse brittle behavior. Wang[13] analyzed dislocation nucleation and emission with a slightly modified Rice framework. The shielding effect and emission criterion of a screw dislocation near an interfacial blunt crack have been studied by Song *et al.*[14]

Furthermore, interface stresses, tension, and energies have been widely used to study the elastic responses of nanoscale structures and elastic fields caused by nanoscale inhomogeneities due to the rapid development of nanotechnology. Studies based upon high resolution electron microscopy proved the occurence of dislocations in nanoscale grains.[15,16] The full dislocations inside the very small grains of nanocrystalline metals have been observed by Wu and Ma.[17] The concept of interface stress in solids was first introduced by Gibbs.[18] Gurtin and Murdoch[19] proposed a mathematical model for elastic isotropic solids incorporating surface/interface stress. Fang and Liu[20] investigated the problem of a screw dislocation inside an inhomogeneity with interface stress.

However, the effect of nano inclusions acting on the interaction between dislocations and cracks has not been studied due to the complexity of the calculation. In the present paper, the interaction between a screw dislocation and a semi-infinite wedge crack with a nano-circular inclusion at the tip is investigated by using the complex variable method.

2. Problem statement and solution

Consider an infinite matrix containing a semi-infinite wedge crack with a nano-circular inclusion at the tip, as shown in Fig. 1(a). A positive screw dislocation of Burgers vector $\boldsymbol{b}_z$ is located at z_0 inside the inclusion. The usual magnitude of the Burgers vector of a screw dislocation is 1 nm, and the range of the size of nano inclusion is $R < 200$ nm. The regions occupied by the nano inclusion and the matrix will be denoted by S^+ and S^-, respectively.

In previous works,[17–19] an interface region was approximated as a vanishing thickness adhering to the bulk solid without slipping. The material constants of the interface are different from the bulk materials. The equilibrium and constitutive equations of the bulk solid are the same as those in the classical elasticity, but the presence of interface stress gives rise to nonclassical boundary conditions. For the current problem, the boundary conditions at the nano-inhomogeneity interface

*Project supported by the Postdoctoral Research Funds of Jiangsu Province, China (Grant No. 1002008B) and the China Postdoctoral Science Foundation (Grant No. 20110491416).

†Corresponding author. E-mail: hpsong@nuaa.edu.cn

© 2013 Chinese Physical Society and IOP Publishing Ltd

can be summarized as[19]

$$w_1^+ = w_1^-, \tag{1}$$

$$\tau_{rz1}^+ - \tau_{rz2}^- = \frac{\mu^0 - \tau^0}{R\mu_1}\frac{\partial \tau_{\theta z1}^+}{\partial \theta}, \tag{2}$$

where μ^0 denotes the interfacial elastic constant, τ^0 is the residual interface tension, and τ_{rz} and $\tau_{\theta z}$ are stress components. Noting that the interface region is approximated as a vanishing thickness, therefore the dimension of μ^0 and τ^0 are N/m,[18] and the units at both sides of Eq. (2) are consistent.

The boundary conditions on the surface of the crack have the form

$$\tau_\perp = 0, \tag{3}$$

where the subscript $\perp$ means perpendicular to the surface.

The antiplane displacement w, shear stresses τ_{rz}, and $\tau_{\theta z}$ can be written in terms of an analytical function $f(z)$ as follows:

$$w = \mathrm{Re}[f(z)], \tag{4}$$

$$\tau_{rz} - \mathrm{i}\tau_{\theta z} = \mu \mathrm{e}^{\mathrm{i}\theta} f'(z), \tag{5}$$

where μ is the shear modulus of the material. Thus, the displacement and stress conditions in Eqs. (1)–(3) can be written as

$$\mathrm{Re}[f_1(z)]^+ = \mathrm{Re}[f_2(z)]^-, \tag{6}$$

$$\mu_1\left[\mathrm{e}^{\mathrm{i}\theta} f_1'(z) + \mathrm{e}^{-\mathrm{i}\theta}\overline{f_1'(z)}\right]^+ + \frac{\mu^0 - \tau^0}{R}\left[\mathrm{e}^{\mathrm{i}\theta} f_1'(z) + \mathrm{Re}^{2\mathrm{i}\theta} f_1''(z) + \mathrm{e}^{-\mathrm{i}\theta}\overline{f_1'(z)} + \mathrm{Re}^{-2\mathrm{i}\theta}\overline{f_1''(z)}\right]^+ = \mu_2\left[\mathrm{e}^{\mathrm{i}\theta} f_2'(z) + \mathrm{e}^{-\mathrm{i}\theta}\overline{f_2'(z)}\right]^-, \tag{7}$$

$$\mathrm{Im}\left[\mu \mathrm{e}^{\mathrm{i}(\pi-\alpha/2)} f'(z)\right] = 0. \tag{8}$$

The following transform function

$$w = \omega(z) = z^{1/m}, \quad z = G(w) = w^m, \tag{9}$$

$$m = \frac{2\pi - \alpha}{\pi}, \quad (1 < m < 2), \tag{10}$$

can map the half plane with a half-circular inclusion (with radius $R' = R^{1/m}$) in the w plane to a circular inclusion (with radius R) with a semi-infinite wedge crack (with radian α) in the z plane (see Fig. 1(b)). Herein, m is the parameter related to the radian of the wedge crack.

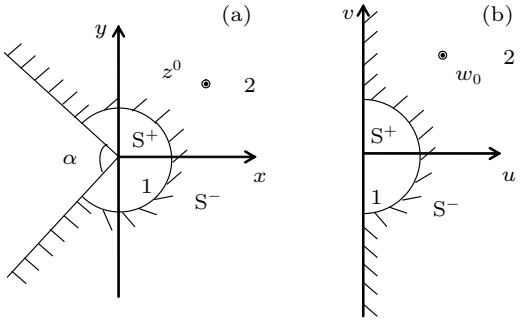


Fig. 1. (a) A screw dislocation near a nano-circular inclusion with a semi-infinite wedge crack. (b) The w plane.

Consequently, the boundary conditions of Eqs. (6)–(8) may be represented as

$$\mathrm{Re}[f_1(w)]^+ = \mathrm{Re}[f_2(w)]^-, \tag{11}$$

$$\mathrm{Re}\left[\mu_1 \mathrm{e}^{\mathrm{i}\theta} f_1'(z)\right]^+ + \frac{\mu^0 - \tau^0}{R}\mathrm{Re}\left[\mathrm{e}^{\mathrm{i}\theta} f_1'(z) + \mathrm{Re}^{2\mathrm{i}\theta} f_1''(z)\right]^+ = \mathrm{Re}\left[\mu_2 \mathrm{e}^{\mathrm{i}\theta} f_2'(z)\right]^-, \tag{12}$$

$$\mathrm{Im}\left[\mu \mathrm{e}^{\mathrm{i}(\pi-\alpha/2)} f'(w)\frac{\mathrm{d}w}{\mathrm{d}z}\right] = 0. \tag{13}$$

Equations (11)–(13) can be further simplified into

$$\mathrm{Re}[f_1(w)]^+ = \mathrm{Re}[f_2(w)]^-, \tag{14}$$

$$\mathrm{Re}\left[\mu_1 w f_1'(w)\right]^+ + \frac{\mu^0 - \tau^0}{Rm}\mathrm{Re}\left[w f_1'(w) + w^2 f_1''(w)\right]^+ = \mathrm{Re}\left[\mu_2 w f_2'(w)\right]^-, \tag{15}$$

$$\mathrm{Im}\left[\mathrm{i} f'(w)\right] = 0. \tag{16}$$

Now, the boundary conditions of Eqs. (14) and (15) are just the same as the problem of a screw dislocation inside a circular nano inclusion,[17] if we replace R and $\mu^0 - \tau^0$ with $R^{1/m}$ and $(\mu^0 - \tau^0)R^{1/m}/(Rm)$, respectively.

Thus, the solutions can be given by

$$f_1'(w) = \frac{b_z}{2\pi\mathrm{i}}\frac{1}{w - w_0} + \frac{2\mu_2\Gamma}{\mu_1 + \mu_2 + (\mu^0 - \tau^0)/Rm} + \frac{b_z}{2\pi\mathrm{i}}\sum_{k=0}^{\infty}\frac{\left[\mu_1 - \mu_2 - (1+k)(\mu^0 - \tau^0)/Rm\right](\bar{w}_0)^{k+1}}{\left[\mu_1 + \mu_2 + (1+k)(\mu^0 - \tau^0)/Rm\right]R^{2(k+1)/m}}w^k, \tag{17}$$

$$f_2'(w) = \frac{b_z}{2\pi\mathrm{i}}\frac{1}{w - w_0} + \Gamma + \frac{\left[\mu_1 - \mu_2 + (\mu^0 - \tau^0)/Rm\right]R^{2/m}\bar{\Gamma}}{\left[\mu_1 + \mu_2 + (\mu^0 - \tau^0)/Rm\right]w^2} + \frac{b_z}{2\pi\mathrm{i}}\sum_{k=0}^{\infty}\frac{\left[\mu_1 - \mu_2 - (1+k)(\mu^0 - \tau^0)/Rm\right](w_0)^{k+1}}{\left[\mu_1 + \mu_2 + (1+k)(\mu^0 - \tau^0)/Rm\right]w^{k+2}}, \tag{18}$$

where $\Gamma = -\mathrm{i}\tau_{yw}^{\infty}/\mu_2$.

Solutions (17) and (18) satisfy boundary conditions (14) and (15), but dissatisfy boundary condition (16). Therefore, an image dislocation with Burgers vector $-b_z$ is put at $-\bar{w}_0$ to make the solution meet the third boundary condition, and the locations of the real dislocation and the image dislocation are symmetric about the free surface.

Finally, the solutions satisfying all the three boundary conditions are

$$f_1'(w) = \frac{b_z}{2\pi\mathrm{i}}\frac{1}{w - w_0} + \frac{2\mu_2\Gamma}{\mu_1 + \mu_2 + (\mu^0 - \tau^0)/Rm} + \frac{b_z}{2\pi\mathrm{i}}\sum_{k=0}^{\infty}\frac{\left[\mu_1 - \mu_2 - (1+k)(\mu^0 - \tau^0)/Rm\right](\bar{w}_0)^{k+1}}{\left[\mu_1 + \mu_2 + (1+k)(\mu^0 - \tau^0)/Rm\right]R^{2(k+1)/m}}w^k$$

$$-\frac{b_z}{2\pi \mathrm{i}}\frac{1}{w+\bar{w}_0}-\frac{b_z}{2\pi \mathrm{i}}\sum_{k=0}^{\infty}\frac{[\mu_1-\mu_2-(1+k)(\mu^0-\tau^0)/Rm](-w_0)^{k+1}}{[\mu_1+\mu_2+(1+k)(\mu^0-\tau^0)/Rm]R^{2(k+1)/m}}w^k, \tag{19}$$

$$\begin{aligned} f_2'(w) = {} & \frac{b_z}{2\pi \mathrm{i}}\frac{1}{w-w_0}-\frac{b_z}{2\pi \mathrm{i}}\frac{1}{w+\bar{w}_0}+\frac{b_z}{2\pi \mathrm{i}}\sum_{k=0}^{\infty}\frac{[\mu_1-\mu_2-(1+k)(\mu^0-\tau^0)/Rm](w_0)^{k+1}}{[\mu_1+\mu_2+(1+k)(\mu^0-\tau^0)/Rm]w^{k+2}} \\ & -\frac{b_z}{2\pi \mathrm{i}}\sum_{k=0}^{\infty}\frac{[\mu_1-\mu_2-(1+k)(\mu^0-\tau^0)/Rm](-\bar{w}_0)^{k+1}}{[\mu_1+\mu_2+(1+k)(\mu^0-\tau^0)/Rm]w^{k+2}}+\Gamma+\frac{[\mu_1-\mu_2+(\mu^0-\tau^0)/Rm]R^{2/m}\bar{\Gamma}}{[\mu_1+\mu_2+(\mu^0-\tau^0)/Rm]w^2}. \end{aligned} \tag{20}$$

With the aid of the mapping functions (9) and (10), the stress field at z due to a screw dislocation at z_0 near a nano-circular inclusion with a semi-infinite wedge crack can be obtained as follows:

$$\begin{aligned} \tau_{xz1}(z)-\mathrm{i}\tau_{yz1}(z) = {} & \frac{\mu_1 \mathrm{d}f_1(z)}{\mathrm{d}z}=\frac{\mu_1 \mathrm{d}f_1(w)}{\mathrm{d}w}\frac{\mathrm{d}w}{\mathrm{d}z} \\ = {} & \frac{w^{1-m}}{m}\frac{\mu_1 b_z}{2\pi \mathrm{i}}\left\{\left(\frac{1}{w-w_0}-\frac{1}{w+\bar{w}_0}\right)+\sum_{k=0}^{\infty}\frac{[\mu_1-\mu_2-(1+k)(\mu^0-\tau^0)/Rm](\bar{w}_0)^{k+1}}{[\mu_1+\mu_2+(1+k)(\mu^0-\tau^0)/Rm]R^{2(k+1)/m}}w^k\right. \\ & \left.-\sum_{k=0}^{\infty}\frac{[\mu_1-\mu_2-(1+k)(\mu^0-\tau^0)/Rm](-w_0)^{k+1}}{[\mu_1+\mu_2+(1+k)(\mu^0-\tau^0)/Rm]R^{2(k+1)/m}}w^k\right\}+\frac{w^{1-m}}{m}\frac{2\mu_1\mu_2\Gamma}{\mu_1+\mu_2+(\mu^0-\tau^0)/Rm}, \end{aligned} \tag{21}$$

$$\begin{aligned} \tau_{xz2}(z)-\mathrm{i}\tau_{yz2}(z) = {} & \frac{\mu_2 \mathrm{d}f_2(z)}{\mathrm{d}z}=\frac{\mu_2 \mathrm{d}f_2(w)}{\mathrm{d}w}\frac{\mathrm{d}w}{\mathrm{d}z} \\ = {} & \frac{w^{1-m}}{m}\frac{\mu_2 b_z}{2\pi \mathrm{i}}\left\{\left(\frac{1}{w-w_0}-\frac{1}{w+\bar{w}_0}\right)+\sum_{k=0}^{\infty}\frac{[\mu_1-\mu_2-(1+k)(\mu^0-\tau^0)/Rm](w_0)^{k+1}}{[\mu_1+\mu_2+(1+k)(\mu^0-\tau^0)/Rm]w^{k+2}}\right. \\ & \left.-\sum_{k=0}^{\infty}\frac{[\mu_1-\mu_2-(1+k)(\mu^0-\tau^0)/Rm](-\bar{w}_0)^{k+1}}{[\mu_1+\mu_2+(1+k)(\mu^0-\tau^0)/Rm]w^{k+2}}\right\} \\ & +\frac{\mu_2 w^{1-m}}{m}\left\{\Gamma+\frac{[\mu_1-\mu_2+(\mu^0-\tau^0)/Rm]R^{2/m}\bar{\Gamma}}{[\mu_1+\mu_2+(\mu^0-\tau^0)/Rm]w^2}\right\}, \end{aligned} \tag{22}$$

where τ_{xz} and τ_{yz} are the perturbation stress components at the dislocation.

It is worth pointing out that for a semi-infinite wedge crack with infinite length, any regular remote loads will lead to an infinite stress intensity factor (SIF). In order to make the SIF produced by the remote loads match the SIF produced by the dislocation, the actual remote loads (Eq. 22) are weakened to $\tau_{xz}^{\infty}-\mathrm{i}\tau_{yz}^{\infty}=\lim_{z\to\infty}(\mu_2 z^{(1-m)/m}\Gamma)/m$, where τ_{xz}^{∞} and τ_{yz}^{∞} are the remote mechanical stress components.

3. Stress intensity factors

The stress intensity factor at the right tip of the wedge crack can be obtained by[21]

$$\begin{aligned} K_{\mathrm{III}} = {} & \lim_{z\to 0}\sqrt{2\pi}z^{(1-1/m)}\sigma_{yz1}=-\mathrm{Im}\left\{\frac{\mu_1 b_z}{m\mathrm{i}\sqrt{2\pi}}\left(\frac{1}{w-w_0}-\frac{1}{w+\bar{w}_0}\right)+\sum_{k=0}^{\infty}\frac{[\mu_1-\mu_2-(1+k)(\mu^0-\tau^0)/Rm](\bar{w}_0)^{k+1}}{[\mu_1+\mu_2+(1+k)(\mu^0-\tau^0)/Rm]R^{2(k+1)/m}}w^k\right. \\ & \left.-\sum_{k=0}^{\infty}\frac{[\mu_1-\mu_2-(1+k)(\mu^0-\tau^0)/Rm](-w_0)^{k+1}}{[\mu_1+\mu_2+(1+k)(\mu^0-\tau^0)/Rm]R^{2(k+1)/m}}w^k\right\}+\frac{\sqrt{2\pi}}{m}\frac{2\mu_1\mu_2\Gamma}{\mu_1+\mu_2+(\mu^0-\tau^0)/Rm}. \end{aligned} \tag{23}$$

The normalized stresses intensity factor produced by the dislocation for different values of μ^0 as a function of R is shown in Fig. 2. It is seen that the stresses intensity factor produced by the dislocation is always negative, which means positive screw dislocations can reduce the SIF of the wedge crack (shielding effect). The shielding effect increases with the increase of μ^0, but decreases with the increase of R. This indicates that the shielding effect produced by the dislocation is enhanced for considering the interface stress, and the size dependence becomes significant when the radius is very small

The curves of variation of SIF produced by the remote load with respect to R at different values of μ^0 are shown in Fig. 3. It is found that the SIF produced by the remote loading is positive. The SIF decreases with the increase of μ^0, but increases with the increase of R, which means the nano inclusion shields the wedge crack so as to consider the effect of the interface stress. Thus, the nano inclusion not only enhances the shielding effect produced by dislocations, but also provides a shielding effect itself. This may be one of the reasons why nano composites have much higher toughness.

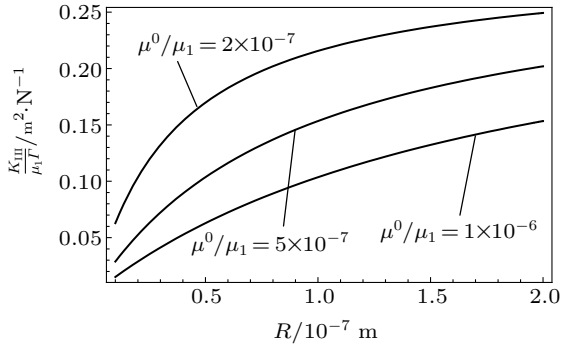


Fig. 2. Curves of normalized SIF versus R with $\mu_2/\mu_1 = 2$, $\alpha = 0.2\pi$, $b_z = 0$, and $\tau^0 = 0$.

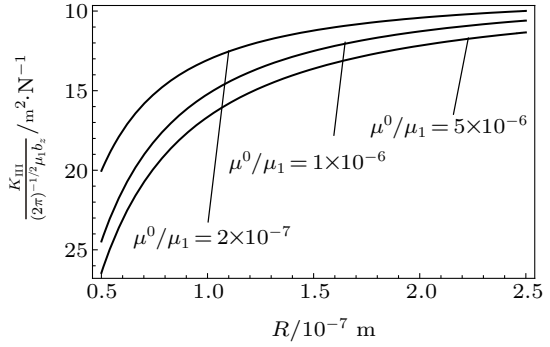


Fig. 3. Curves of normalized SIF versus R with $\mu_2/\mu_1 = 2$, $\alpha = 0.2\pi$, $z_0 = 9.8\times10^{-8}$, $\tau^0 = 0$, and $\Gamma = 0$.

4. Image force

The image force acting on the screw dislocation can be written as

$$F_x - \mathrm{i}F_y = \mathrm{i}b_z\left[\tau_{xz}(w_0) - \mathrm{i}\,\tau_{yz}(w_0)\right], \tag{24}$$

where $\tilde{\tau}_{xz}(z_0)$ and $\tilde{\tau}_{yz}(z_0)$ are the components of the perturbation stress, and F_x and F_y are the force components on the dislocation.

Substituting Eq. (21) into Eq. (24) yields

$$\begin{aligned} F_x - \mathrm{i}F_y = {} & \frac{w^{1-m}}{m}\frac{\mu_1 b_z^2}{2\pi}\left\{-\frac{1}{w+\bar{w}_0} + \sum_{k=0}^{\infty}\frac{\left[\mu_1-\mu_2-(1+k)(\mu^0-\tau^0)/Rm\right](\bar{w}_0)^{k+1}}{\left[\mu_1+\mu_2+(1+k)(\mu^0-\tau^0)/Rm\right]R^{2(k+1)/m}}w^k\right. \\ & \left. - \sum_{k=0}^{\infty}\frac{\left[\mu_1-\mu_2-(1+k)(\mu^0-\tau^0)/Rm\right](-w_0)^{k+1}}{\left[\mu_1+\mu_2+(1+k)(\mu^0-\tau^0)/Rm\right]R^{2(k+1)/m}}w^k\right\} + \frac{\mathrm{i}b_z w^{1-m}}{m}\frac{2\mu_1\mu_2\Gamma}{\mu_1+\mu_2+(\mu^0-\tau^0)/Rm}. \end{aligned} \tag{25}$$

Figures 4 and 5 show the normalized image force $F_x(2\pi/(\mu_1 b_z^2))$ versus z_0/R and R at different values of μ_0, repectively. It is seen that an additional repulsive force will act on the screw dislocation to consider the interface stress. Thus, dislocations may be trapped in the nano inclusion even when the matrix is softer than the inclusion. This helps dislocation shields crack, and reduces the dislocation density within the matrix.

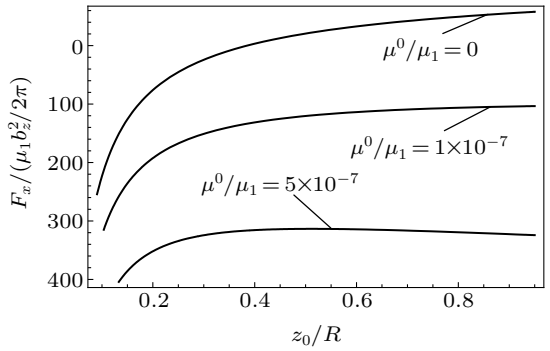


Fig. 4. Curves of normalized image force versus z_0/R with $\mu_2/\mu_1 = 0.7$, $\alpha = 0.2\pi$, $R = 10^{-7}$, $\tau^0 = 0$, and $\Gamma = 0$.

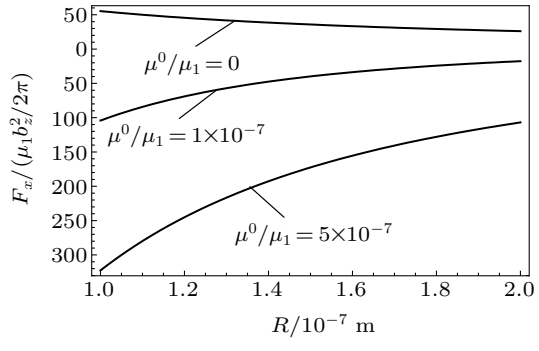


Fig. 5. Curves of normalized image force versus R with $\mu_2/\mu_1 = 0.7$, $\alpha = 0.2\pi$, $z_0 = R - 10^{-8}$, $\Gamma = 0$, and $\tau^0 = 0$.

5. Dislocation emission

For a screw dislocation slip on a plane denoted by the angle θ, the slip force acting on the screw dislocation can be written as

$$\begin{aligned} F_{\mathrm{emit}} &= F_x\cos\theta + F_y\sin\theta \\ &= \mathrm{Re}\left[F_{\mathrm{imag}} + F_\Gamma\right]\cos\theta - \mathrm{Im}\left[F_{\mathrm{imag}} + F_\Gamma\right]\sin\theta, \end{aligned} \tag{26}$$

where F_Γ denotes the image force produced by the remote mechanical stress σ_{23}^{∞}, and F_{imag} denotes the image force produced by the nano inclusion and the wedge crack.

A commonly accepted criterion for the emission of dislocation monopoles from a crack tip is that the force applied on them is equal to zero. Moreover, the dislocation distance to the crack surface must be equal or larger than the dislocation core radius.[10] In the present work, the similar assumption is valid and $z_0 = b_z(\cos\theta + \mathrm{i}\sin\theta)$ sets the condition for the emission of screw dislocation. Based on Eqs. (24)–(26), the critical applied stress and the critical electric displacement for the dislocation emission can be obtained

$$A\sigma_{32}^{\infty} = \sin\theta\,\mathrm{Im}\left[F_{\mathrm{imag}}(z_0)\right] - \cos\theta\,\mathrm{Re}\left[F_{\mathrm{imag}}(z_0)\right], \tag{27}$$

where

$$A = \mathrm{Re}\left[\frac{b_z}{m} z_0^{(1-m)/m} \frac{2\mu_1\mu_2}{\mu_1+\mu_2+(\mu^0-\tau^0)/Rm}\right]\cos\theta$$
$$-\mathrm{Im}\left[\frac{b_z}{m} z_0^{(1-m)/m} \frac{2\mu_1\mu_2}{\mu_1+\mu_2+(\mu^0-\tau^0)/Rm}\right]\sin\theta.$$

The curves of variation of critical load σ_{32}^{∞} with respect to θ at different values of μ^0 are shown in Fig. 6. It is seen that the critical load increases with the increase of μ^0 and α, which means the increase of the crack angle and the existence of interface stress makes dislocation emission more difficult.

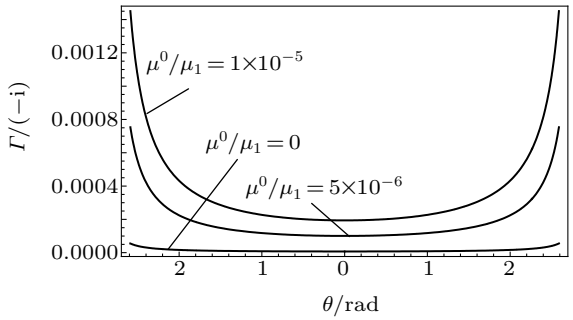


Fig. 6. Curves of normalized critical load versus θ with $\mu_2/\mu_1 = 1.2$, $\alpha = 0.2\pi$, $R_1 = 10^{-7}$, and $\tau^0 = 0$.

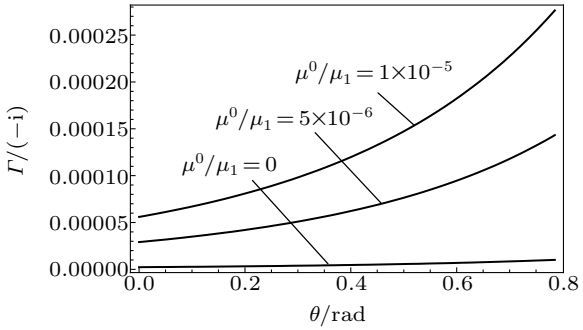


Fig. 7. Curves of normalized critical load versus α with $\mu_2/\mu_1 = 1.2$, $\theta = 0$, $R = 10^{-7}$, and $\tau^0 = 0$.

6. Conclusions

The closed-form solutions of the stress fields in the matrix and the inclusion region are derived. The stress intensity factor, the image force, as well as the critical loads for dislocation emission are discussed in detail. In summary, the following conclusions have been obtained:

(i) The results show that the nano inclusion not only enhances the shielding effect exerted by the dislocation, but also provides a shielding effect itself.

(ii) An additional repulsive force will act on the screw dislocation so as to consider the interface stress. Hence, dislocations may be trapped in the nano inclusion, even the matrix is softer than the inclusion. This helps dislocation shields crack, and reduces the dislocation density within the matrix.

(iii) The increases of the crack angle and the existence of interface stress make dislocation emission more difficult.

References

[1] Zhang T Y and Li J C M 1992 *J. Appl. Phys.* **72** 2215
[2] Zhang T Y and Tong T 1995 *J. Appl. Phys.* **78** 4873
[3] Lin I H and Thomson R 1986 *Acta Metall.* **34** 187
[4] Song H P and Gao C F 2011 *Meccanica* **47** 1097
[5] Shiue S T 1997 *Mater. Chem. Phy.* **48** 220
[6] Zhu T, Li J and Yip S 2004 *Phys. Rev. Lett.* **93** 025503
[7] Fang Q H, Liu Y W and Jiang C P 2003 *Int. J. Struct. Solids* **40** 5781
[8] Fan T Y, Guo R P and Liu G T 2003 *Chin Phys.* **12** 1149
[9] Jin B, Fang Q H and Liu Y W 2007 *Acta. Mech. Solida. Sin.* **20** 50
[10] Tanguy D, Razafindrazaka M and Delafosse D 2008 *Acta Mater.* **56** 2441
[11] Weertman J 1996 *Dislocation Based Fracture Mechanics* (Singapore: World Scientific)
[12] Rice J R and Thomson R 1974 *Philos. Mag.* **29** 73
[13] Wang T C 1995 *Int. J. Fracture* **69** 295
[14] Song H P, Fang Q H and Liu Y W 2009 *Chin. Phys.* B **18** 1564
[15] Wunderlich W, Ishida Y and Maurer R 1990 *Scripta Metall. Mater* **24** 403
[16] Li D X, Ping D H, Ye Q H, Qin X Y and Wu X J 1993 *Mater. Lett.* **18** 29
[17] Wu X L and Ma E 2006 *Appl. Phys. Lett.* **88** 231911
[18] Gibbs J W 1928 *The Collected Works of J. Willard Gibbs* (New York: Longmans, Green and Co.)
[19] Gurtin M F and Murdoch A I 1975 *Arch. Rat. Mech. Anal.* **57** 291
[20] Fang Q H and Liu Y W 2007 *Mater. Sci. Eng.* A **464** 117
[21] Ohr S M, Chang S J and Thomson R 1985 *J. Appl. Phys.* **57** 1839